Water Research 288 (2026) 124705

Contents lists available at ScienceDirect

Water Research

journal homepage: www.elsevier.com/locate/watres

Mechanical resistance of higher EPS contents in larger granules restricts anammox bacterial growth

Dongdong Xu [a,b], Tao Liu [c], Jiahui Fan [b], Wenda Chen [a], Yiyu Li [a], Meng Zhang [a,*], Ping Zheng [a], Jianhua Guo [b,*]

[a] Department of Environmental Engineering, College of Environmental & Resource Sciences, Zhejiang University, Hangzhou 310058, China
[b] Australian Centre for Water and Environmental Biotechnology, The University of Queensland, St. Lucia, Queensland 4072, Australia
[c] Department of Civil and Environmental Engineering, The Hong Kong Polytechnic University, Hung Hom, Kowloon, Hong Kong 999077, China

HIGHLIGHTS

- Larger anammox granules with higher EPS showed the slower bacterial growth;
- Reduced growth yield in larger granules mainly accounted for slower bacterial growth rate;
- Greater EPS mechanical strength in large granules restricted bacterial growth;
- Ultrasound improved bacterial growth yield by loosening dense EPS structure in larger granules.

GRAPHICAL ABSTRACT

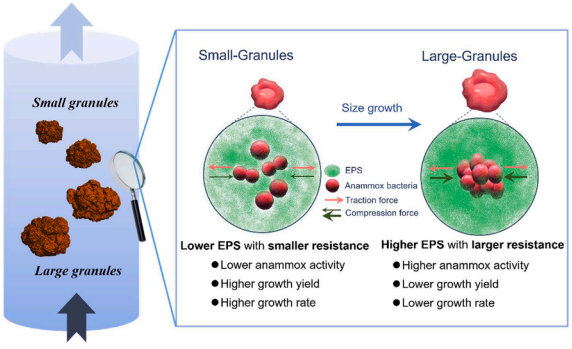

ARTICLE INFO

Keywords:
EPS
Microbial granule
Anammox bacteria
Growth
Physical and mechanical resistances

ABSTRACT

Extracellular polymeric substances (EPS) are core granular components, playing critical roles in its structural stability. However, little is known about the effect of EPS on bacterial growth due to physical and mechanical resistances posed by EPS matrix. Herein, anaerobic ammonium oxidation (anammox) granules with different sizes and EPS contents were collected from a full-scale plant. Using ^{13}C isotope labelling and qPCR assays, we confirmed that larger granules with higher EPS content exhibited the higher maximum nitrogen removal activity but much lower bacterial growth yield, resulting in a significantly lower maximum specific growth rate (-26.8%), compared to smaller granules. Metagenomic sequencing revealed that anammox species were identical in different granules, and actual EPS production yields were similar in 15-day incubation, ruling out the possibility that more energy was diverted to produce additional EPS in larger granules. Interestingly, the EPS mechanical strength was significantly greater in large granules, which reduced cell membrane fluidity and severely deformed bacterial cells. These mechanical constraints imposed by the dense EPS matrix limited anammox bacterial proliferation and reduced their growth yield. Using low-intensity ultrasound to loosen EPS structure improved the growth yield of anammox bacteria in large granules, while also enhancing nitrogen removal activity. These together contributed to a substantial increase in bacterial growth rate (+153.3%). The findings highlight that

* Corresponding authors.
E-mail addresses: zhangm_environment@zju.edu.cn (M. Zhang), jianhua.guo@uq.edu.au (J. Guo).

https://doi.org/10.1016/j.watres.2025.124705
Received 17 August 2025; Received in revised form 29 September 2025; Accepted 30 September 2025
Available online 1 October 2025

physical and mechanical resistance imposed by EPS plays a previously overlooked role in bacterial growth, and provide the basis for promoting anammox bacterial proliferation within granules.

1. Introduction

Anaerobic ammonia oxidation (anammox) is a key process in the natural nitrogen cycle and plays a critical role in nitrogen management within artificial systems (Yang et al., 2015; Liu et al., 2024). Anammox bacteria, which drive this process, commonly exist in the form of biofilms (Li Wong et al., 2023). Specifically, in wastewater treatment reactors, anammox bacteria are found to be prone to form granules (Hou et al., 2015; Boleij et al., 2018). Granules, a form of non-attached biofilm with size of approximately 0.2-6 mm, have been widely applied in sustainable wastewater treatment and biobased resource recovery (Mishima and Nakamura, 1991; Pronk et al., 2015). Granules are denser and more compact than flocs, requiring a less surface area and lower upfront capital costs for granule-based bioreactors (Liu and Tay, 2004). Moreover, granules generally settle faster than flocs, thus enabling a high biomass concentration (Wilén et al., 2018). Therefore, granule-based anammox process has been proposed as a sustainable nitrogen removal technology, gaining wide attention due to their advantages in improving treatment efficacy, saving cost, and reducing carbon footprint (Kartal et al., 2010).

Extracellular polymeric substances (EPS), mainly including proteins (PN) and polysaccharides (PS), are proven to play key roles in the granulation of anammox sludge (Boleij et al., 2018). The abundant hydrophobic groups and relatively loose secondary structures of PN enhance hydrophobic interactions, thereby promoting sludge aggregation (Hou et al., 2015). The stability of AnGS could be sharply reduced after hydrolysis of the PN with the protease (Lin and Wang, 2017). PS contain functional groups such as carboxyl and hydroxyl groups that carry negative charges, which facilitate bridging effects and consequently contribute to the granulation of anammox sludge. Also, the properties of the PS chains, such as the degree of branching and the width and height of the chains, were reported to be positively correlated with granular stability (Wang et al., 2020a). All these previous studies consistently showed the positive roles of EPS in maintaining the stability of anammox granular structure. Therefore, most of previous studies aimed to promote the microbial secretion of EPS to obtain the AnGS with a more stable structure and larger size, thus retaining more anammox bacteria and achieving efficient nitrogen removal (Li et al., 2021; Wang et al., 2022; Dsane et al., 2023). Nonetheless, it has been reported that large granules exhibit poor biomass growth performance, suggesting that pursuing larger granules may have inherent limitations (Liu et al., 2005). This reduced growth performance was generally attributed to mass transfer limitations caused by the denser EPS contents and lower specific surface area of large granules, which ultimately suppress bacterial activity (Xu et al., 2021; Peng et al., 2025).

Notably, EPS might play multiple roles in bacterial growth, which have been overlooked in previous studies. For example, a previous study documented that the synthesis and secretion of EPS would consume substantial energy, which could potentially result in less energy available for the synthesis of other essential compounds (e.g., nucleotides), thus limiting the growth of anammox bacteria (Zhao et al., 2023). In addition, cell division requires spatial expansion from a microscopic point of view, while EPS, which typically surround bacterial cells, could impose mechanical resistance to growth (Even et al., 2017; Liu et al., 2022). During proliferation, bacteria generate traction force to drive cell division. When the traction force exceeds the external resistance, the division proceeds smoothly. However, studies have shown that cell growth may be inhibited when the strength of the extracellular matrix exceeds a threshold (Chaudhuri et al., 2020; Saraswathibhatla et al., 2023). Considering that anammox bacterial cells are ensconced within a three-dimensional matrix of EPS (Lin and Wang, 2017), we hypothesized that the strength of EPS might influence the bacterial growth due to physical and mechanical constraints. Although these potential impacts of EPS on anammox bacterial proliferation are critically important, no effort has been made to address this research question in literature.

This study aims to fill this knowledge gap and provide an in-depth understanding of the impacts of EPS on anammox bacterial growth in granules. Given that larger granules usually have more EPS, two types of AnGS (including S-Granules with small size (0.2-2.0 mm) and L-Granules with large size (>2.0 mm)) with different EPS contents were obtained by the size screening. The objectives were (1) to determine the maximum specific growth rate of anammox bacteria in these two types of AnGS using ^{13}C isotope labelling in conjunction with qPCR; (2) to examine the functional anammox species, EPS production yield, and EPS strength, potential factors affecting the growth of anammox bacteria in granules using metagenomic analysis, elastic modulus measurement, and a series of batch experiments; (3) to investigate the microstructure of granules and bacterial cells by monitoring the cell shape and division and measuring the cell membrane fluidity; (4) to confirm the role of EPS by regulating its content through the low-intensity ultrasonic treatment. The findings were expected to offer new insights into the role of EPS in anammox bacterial growth within granules.

2. Materials and methods

2.1. Anammox granules collection

The AnGS used in this study was collected from a full-scale industry wastewater treatment plant employing anammox-based process in Jiangsu Province, China, which has been stably operated for over two years. The plant was dedicated to treating the high-ammonia wastewater generated from the photovoltaic manufacturing process, using a one-stage partial-nitritation and anammox process. The influent ammonium concentration was ~1400 mg-N/L without nitrite and nitrate. The TN loading rate (NLR) and the TN removal efficiency (NRE) were ~0.5 kg-N/(m^3·d) and ~80.0%, respectively. In this system, ammonium-oxidizing bacteria (AOB) mainly existed in the flocs while anammox bacteria mainly lived in the microbial granules. The VSS (Volatile suspended solids) concentration and VSS/TS (Total solids) ratio of AnGS were ~1.2 g/L and 0.91, respectively. Based on differences in granular EPS contents (Fig. S1), the collected AnGS was classified into two groups: S-Granules with small size (0.2-2.0 mm) and L-Granules with large size (>2.0 mm). Specifically, a 2.0 mm pore-size sieve was used to separate the AnGS, and the size distribution of S-Granules and L-Granules was subsequently determined (Fig. S2).

2.2. Anammox bacterial growth yield and maximum N removal rate

2.2.1. Determination of anammox bacterial growth yield

Two different approaches, i.e., ^{13}C isotope labelling and qPCR, were applied to determine the net growth rate of anammox bacteria in AnGS. First, the N-free medium was prepared with the ^{13}C isotope labelled carbon sources including sodium bicarbonate and potassium bicarbonate (Cambridge Isotope Laboratories, 99 ATM%, USA) (Table S1). Approximately 5.0 g AnGS was washed three times using the N-free medium (Table S2). The washed AnGS was transferred to a serum bottle containing 100 mL of N-free medium. Then, argon gas was used to sparge the serum system for 15 min to eliminate the oxygen, and the pH of the mixture was adjusted to 7.8~8.0 with the HCl solution (2 M). After sealing the serum bottle, 1.0 mL of ammonium (5 g-N/L) and nitrite (6 g-N/L) stock solution was injected into the sealed serum bottle through the rubber stopper using a syringe, respectively. The serum

bottle was incubated at 30±1°C on a shaker at 120 rpm for 15 days. The ammonium and nitrite concentrations in serum bottles were measured approximately every 6 hours, and stock solution was dosed accordingly to maintain desired level. Due to the consumption of carbon sources during the experimental period, $^{13}CO_2$ (at normal pressure) was supplemented as needed. Considering the alkalinity generated by anammox reaction, HCl (2 M) was added to accurately adjust the pH of the batch solution to the desired level.

The biomass in the serum bottle was filtered by a 0.45 μm filter membrane after cultivation, and the collected biomass was washed three times with the deionized water. Then, the washed biomass was transferred to a 5 mL centrifuge tube, precooled at -80°C for 24 h, and lyophilized for 48 h. The dried sample was weighed and ground into fine powders, which were collected by passing through a sieve with 160 mesh. Afterwards, the C content and the $\delta^{13}C$ value (Permillage deviation of the ^{13}C to ^{12}C stable isotope ratio in the sample relative to that of the standard) of the powders were detected using an elemental analyser-isotope ratio mass spectrometer (vario MICROcube-IsoPrime 100). The cell growth yield was further calculated according to the Eq. shown in Text S1. To validate the growth rate determined by the ^{13}C isotope labelling method, another complementary approach was further conducted based on monitoring the variation of anammox bacterial 16S rRNA gene using qPCR. The detailed procedures for qPCR assay were presented in Text S2.

2.2.2. Determination of maximum N removal rate

The specific nitrogen removal activity of AnGS was further examined under different substrate concentrations. Specifically, about 1.0 g of AnGS was weighed and washed three times using the N-free medium (Table S2). The washed AnGS were transferred to a serum bottle containing 50 mL of medium. The mixed gas of CO_2 and argon was applied to flush the serum system for 10 min to eliminate the oxygen. After sealing, the initial ammonium was adjusted to 5, 10, 50, 150, 300 and 400 mg-N/L, with a nitrite to ammonium ratio of 1.2. The tests were conducted in a shaker at 120 rpm and a constant temperature of 30°C. Samples of 1.0 mL were collected hourly, and the SAA was calculated based on the sum of ammonium, nitrite, and nitrate removal rates per VSS. Subsequently, the graph of SAA versus substrate concentration was plotted, and the maximum specific nitrogen removal rate was obtained by Haldane model (Eq. 1). Based on the obtained anammox bacterial growth yield and maximum nitrogen removal rate, the maximum specific growth rate of anammox bacteria in AnGS was calculated (Text S1). The procedures for determination of the decay coefficient of anammox bacteria in AnGS were shown in Text S3. All tests described in this section were performed in triplicate.

$$q = \frac{q_{\max}}{1 + \frac{K_s}{S} + \frac{S}{K_i}} \quad (1)$$

Where, q is specific nitrogen removal rate (mg-N/(g-VSS·d)); q_{max} is maximum specific nitrogen removal rate (mg-N/(g-VSS·d)); S is substrate concentration (mg-N/L); K_s is half-saturation constant (mg-N/L); K_i is inhibition constant (mg-N/L).

2.3. Microstructure observation

Transmission electron microscope (TEM, Hitachi H-7650) was applied to observe the microstructure of AnGS and anammox bacteria. Granules were placed in 2.5% glutaraldehyde solution and fixed overnight at 4°C. The samples were fixed using osmium acid solution for 1-2 h after rinsing with phosphate buffer solution (0.1 M, pH 7.0). Subsequently, the fixed samples were rinsed with phosphoric acid buffer again, and then dehydrated with gradient concentration of ethanol solution (50%, 70%, 80%, 90%, 95%, 100%). The samples were then treated with acetone for 20 min, and with a mixture of embedding medium (Spurr) and acetone with volume ratio of 1:1 and 3:1 for 1 h and 3 h, respectively. Afterwards, the samples were processed with the pure embedding medium (Spurr) overnight. The embedded samples were sectioned by the ultra-microtome (LEICA EM UC7), obtaining 70-90 nm sections. The sections were stained with lead citrate and 50% ethanol-saturated uranyl acetate for 5-10 min each, followed by the observation under the Hitachi H-7650 TEM.

2.4. Physicochemical properties characterization

The size of AnGS was determined by the QICPIC dynamic image system (Sympatec GmbH, Germany). The EPS of AnGS was extracted by modified heat extraction method, and the detailed determination procedure was provided in Text S4. The extracellular PN around cells were stained with the Fluorescein isothiocyanate (FITC), and their distribution was observed by a CLSM (LSM780, Zeiss, Germany) under the excitation and emission wavelengths of 488 nm and 500-550 nm. The determination of the actual EPS production yields of AnGS was presented in Text S5. The elastic modulus (Young's modulus, E) of AnGS was detected using an atomic force microscope (AFM), the details were shown in Text S6.

2.5. Metagenomic sequencing and bioinformatics

The total genomic DNA was extracted using DNeasy PowerSoil Kit (QIAGEN GmbH, Germany) based on the manufacturer protocol. The Shotgun library construction (2 × 150 bp) was performed using the extracted DNA samples. Then, Illumina high-throughput sequencing was conducted on Illumina Hiseq 2500 platform at Major Co., Ltd. (Shanghai, China). The raw data quality was confirmed using FastQC. The partial primers and adapters were trimmed from the raw reads using SeqPrep version 1.1. The trimmed sequences were quality filtered using Sickle version 1.33. The contigs were assembled individually using IDBA-UDNext (Peng et al., 2012). After quality control, sequencing of DNA extracted from L-Granules and S-Granules yielded a total of 83,346,828 and 86,239,006 raw reads and 85,260,286 and 82,226,192 clean reads, respectively. Next, the clean reads were assembled, and 504,251 and 521,946 contigs were generated with N50 of 1367 bp and 1329 bp. The ORFs of contigs obtained from splicing results were predicted using MetaGene. Genes with nucleic acid lengths≥100 bp were selected and translated into amino acid sequences. The predicted genetic sequences from all samples were clustered using CD-Hit version 4.8.1 (90% identity and 90% coverage) (Fu et al., 2012). The longest gene in each cluster was then designated as the representative sequence to generate the non-redundant gene set. High-quality reads from each sample were aligned with this non-redundant gene set using SOAPaligner version 2.21 (95% identity) (Li et al., 2008), gene abundance information in each sample was tallied, amino acid sequences of the non-redundant gene set were aligned with the NR database using Diamond with e-value of $1 \times e^{-5}$. The species annotation was obtained by taxonomic information databases, and the species abundance was calculated based on the sum of genes abundances corresponding to each species. The raw sequencing reads of bacterial communities in this study have been deposited into the NCBI Sequence Read Archive (SRA) under the accession number PRJNA1166981.

2.6. Other measurements

The ammonium, nitrite, nitrate, and VSS concentrations were all examined based on the standard methods (Baird et al., 2017). Laurdan dye staining was used to determine the membrane fluidity of anammox bacteria following Wenzel et al. (2018). An ultrasonic cleaning machine (KUDOS, Shanghai) was used to investigate the nitrogen removal activity of L-Granules under different ultrasonic power levels and durations (Text S7). The growth of anammox bacteria in L-Granules treated under the optimal ultrasonic parameters was further evaluated. Moreover, the effect of identical ultrasonic treatment on suspended anammox

bacteria was examined, as detailed in Text S7.

2.7. Statistical analysis

The error bars in this study represent the standard deviation from at least three biological replicates. The statistical significance of the data between different groups was determined with the one-way analysis of variance. The SPSS 22.0 software was employed for statistical analyses. Differences with $p<0.05$ were considered statistically significant.

3. Results

3.1. Activities and growth of anammox bacteria in two different anammox granules

S-Granules and L-Granules were obtained from a full-scale anammox reactor with stable and efficient performance. Compared with S-Granules, L-Granules with a larger size (2.2±0.1 vs 1.4±0.1 mm, +57.7%, $p<0.001$), contain significantly higher EPS content (244.2±21.8 vs 163.5±19.6 mg/g-VSS, +49.4%, $p<0.01$) (Fig. 1A, B). This was in line with previous studies showing that granules with the larger size commonly have higher EPS content, which is conducive to their structural stability (Wang et al., 2020b; Xu et al., 2021). Moreover, L-Granules accounted for the dominant percentage of over 75% in biomass, while the proportion of S-Granules was ~20% (Fig. 1C).

The maximum specific nitrogen conversion rates of S-Granules and L-Granules were investigated (Fig. 2A, B). The maximum specific TN and ammonium removal rates of S-Granules were 501.2±19.7 and 259.7 ±12.8 mg-N/(g-VSS·d), respectively. In contrast, L-Granules exhibited significantly higher rates of 778.9±26.9 and 397.4±18.9 mg-N/(g-VSS·d), respectively ($p<0.001$) (Fig. 2C). Subsequently, the anammox bacterial growth yields of S-Granules and L-Granules were determined to be (6.2±0.4) × 10^{-2} and (2.9±0.2) × 10^{-2} g-C/g-NH_4^+-N, respectively, using the ^{13}C isotope-labelled experiments (Fig. 2D). To ensure the reliability of obtained results, the qPCR-based quantification was further used to investigate the anammox bacteria growth yields. The qPCR-based quantification showed anammox bacteria growth yields of (7.2 ±0.5) × 10^{10} and (4.8±0.3) × 10^{10} copies/g-NH_4^+-N for S-Granules and L-Granules, respectively (Fig. 2D).

Based on the obtained maximum specific nitrogen removal rate and growth yield, the maximum specific growth rate of anammox bacteria was further calculated. According to the data from the ^{13}C isotope-labelled experiment, the maximum specific growth rates of anammox bacteria in S-Granules and L-Granules were (4.1±0.2) × 10^{-2} d^{-1} and (3.0 ±0.2) × 10^{-2} d^{-1}, respectively, corresponding to doubling times of 17.0 ±1.5 d and 22.9±1.2 d (Fig. 2E, F). Similarly, the qPCR-based method yielded maximum specific growth rates of (4.3±0.2) × 10^{-2} d^{-1} and (3.1 ±0.2) × 10^{-2} d^{-1} for S-Granules and L-Granules, respectively, with doubling times of 16.0±1.4 d and 22.3±1.6 d (Fig. 2E, F). Notably, the maximum specific growth rates and doubling times obtained by the two methods were consistent, underscoring the reliability of the determined results.

It should be noted that the maximum specific ammonium removal rate of L-Granules was 1.53-fold higher than S-Granules ($p<0.001$). However, the actual growth yield of anammox bacteria in L-Granules was much lower than that in S-Granules, with reductions of 53.2% as determined by the ^{13}C isotope-labelling tests and 33.3% by qPCR-based assay. The lower growth yield resulted in the significantly lower maximum specific growth rate (-26.8% and -29.3%) and longer doubling time of anammox bacteria in L-Granules ($p<0.001$). These results collectively showed that the biomass yield and bacterial growth rate of large granules were significantly lower than small granules, although they exhibited higher nitrogen removal rates.

3.2. Functional microorganisms and EPS in two different anammox granules

3.2.1. Species and abundance of anammox bacteria

In order to test whether the disparity of growth yields observed in S-Granules and L-Granules was caused by different anammox species, we employed metagenomic sequencing to examine the functional anammox species in different granules. Based on taxonomic analysis, we found that *"Ca. Brocadia sapporoensis"* was the sole anammox bacteria species detected in both S-Granules and L-Granules (Fig. 3A). Therefore, the observed lower growth yield of anammox bacteria in L-Granules was not related to the difference in anammox species. Notably, the relative abundance of *"Ca. Brocadia sapporoensis"* in S-Granules was 38.7%, while it reached 62.4% in L-Granules. The quantitative results by qPCR also corroborated that L-Granules harbored significantly more anammox bacteria ($p<0.01$) (Fig. 3B). The higher abundance of anammox bacteria of L-Granules was correlated with the higher nitrogen removal rate observed (Fig. 2C). Potential heterotrophic denitrifiers, including *Anaerolineae_bacterium, Chloroflexi_bacterium, Proteobacteria_bacterium*, and *Rhodocyclaceae_bacterium* were detected in both S-Granules and L-Granules (Fig. 3A). These microorganisms were likely sustained by cell lysis products or carbon compounds excreted by other microbes (Lawson et al., 2017), and showed comparable abundances in both types of granules.

3.2.2. EPS production and structural strength of EPS

Bacterial growth is closely related to the cellular energy levels. The ATP content in S-Granules was 60.5±4.3 μmol/g-VSS, which was significantly higher than that in L-Granules (47.1±3.9 μmol/g-VSS, $p<0.05$) (Fig. S3). Since EPS synthesis requires substantial energy (Zhao

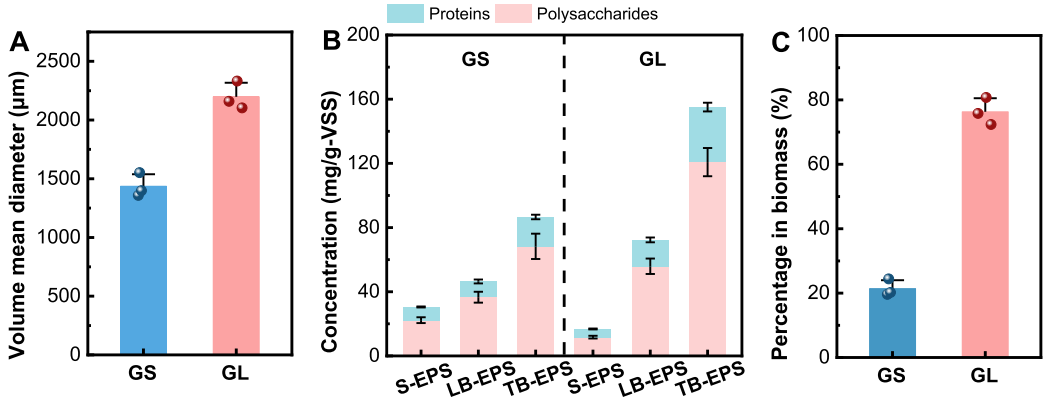

Fig. 1. Comparison of size (A), EPS content (B) and biomass percentage (C) between S-Granules and L-Granules. S-EPS, LB-EPS and TB-EPS refer to soluble, loosely bound and tightly bound EPS, respectively. GS and GL refer to S-Granules and L-Granules, respectively, and the same as below.

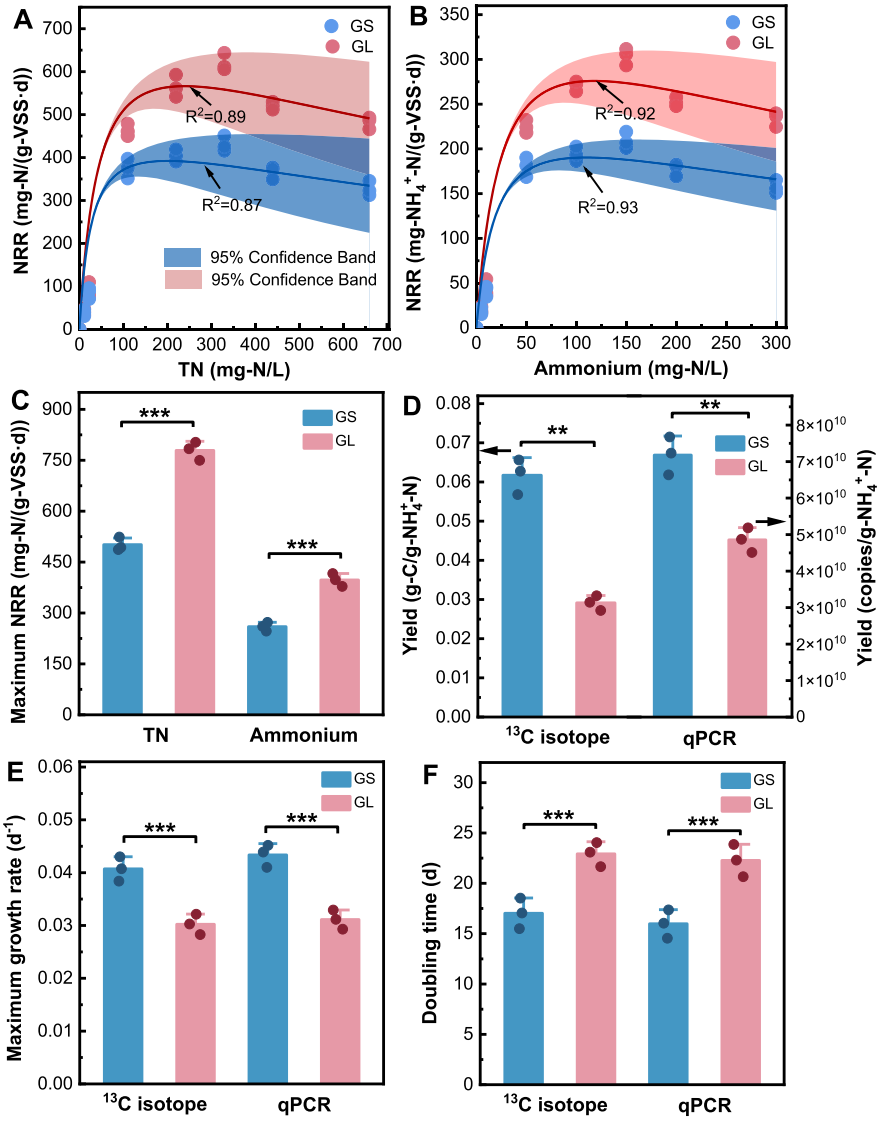

Fig. 2. Comparison of anammox activities and growth between S-Granules and L-Granules. Total nitrogen (TN) (A) and ammonium (B) utilization kinetic curves of S-Granules and L-Granules. Maximum specific TN, ammonium removal rates (C) and anammox bacterial growth yields (D) of S-Granules and L-Granules; Maximum specific growth rates (E) and doubling time (F) of anammox bacteria in S-Granules and L-Granules. ^{13}C isotope and qPCR refer to two measurement methods of growth yield. Significant differences were detected using one-way analysis of variance: * $p<0.05$, ** $p<0.01$, and *** $p<0.001$.

et al., 2023), we tested whether the lower growth yield of anammox bacteria in L-Granules was related to the higher generation yield of EPS. The measured EPS production yields of S-Granules and L-Granules were 31.6±3.6 and 28.8±3.9 mg/g-NH_4^+-N, respectively, showing no significant differences during the experimental period ($p>0.05$, Fig. 3C). These results suggest that the difference in the EPS production yield is not the primary cause for the significant discrepancy in the growth yield of anammox bacteria in S-Granules and L-Granules.

Further, we evaluated the strength of EPS in different granules, which was reflected by the elastic modulus measured by atomic force microscopy (Jorba et al., 2017). It was found that the elastic modulus of L-Granules was significantly higher than that of S-Granules (113.9 vs 68.7 Mpa, +65.8%, $p<0.001$) (Fig. 3D-G), highlighting the greater structural strength of EPS in L-Granules. This was closely associated with the higher EPS content in L-Granules. Specifically, L-Granules contained significantly higher levels of both loosely bound EPS (LB-EPS) and tightly bound EPS (TB-EPS) compared to S-Granules (Fig. S4), with both positively correlating with the elastic modulus. Therefore, we hypothesized that the EPS with a higher content and a greater structural strength in L-Granules might have exerted a greater resistance to the anammox bacterial growth.

3.3. Microstructure of granules and bacterial cells

To elucidate the significant growth resistance faced by anammox bacteria in L-Granules, the microstructure of granules was further examined. In S-Granules, the anammox bacterial density was relatively lower, displaying a more dispersed distribution pattern (Fig. 4A, B). Additionally, the electron density surrounding the cells was less pronounced, which was in line with the lower anammox bacteria count and less EPS content in S-Granules (Figs. 3B, 4M). Further observations suggested that most of the anammox bacterial cells in S-Granules were round and in full size (Fig. 4C). A large number of dividing cells were observed in S-Granules, suggesting the higher maximum growth rate of anammox bacteria (Fig. 4D-F). Notably, anammox bacteria proliferated in a two-division process, including the mother cell grows up and then divides into two daughter cells with equal size and shape (Weiss, 2004). This was in accordance with the previously reported results (Van Niftrik et al., 2009). In contrast, L-Granules exhibited a markedly higher density of anammox bacterial cells with a more concentrated distribution

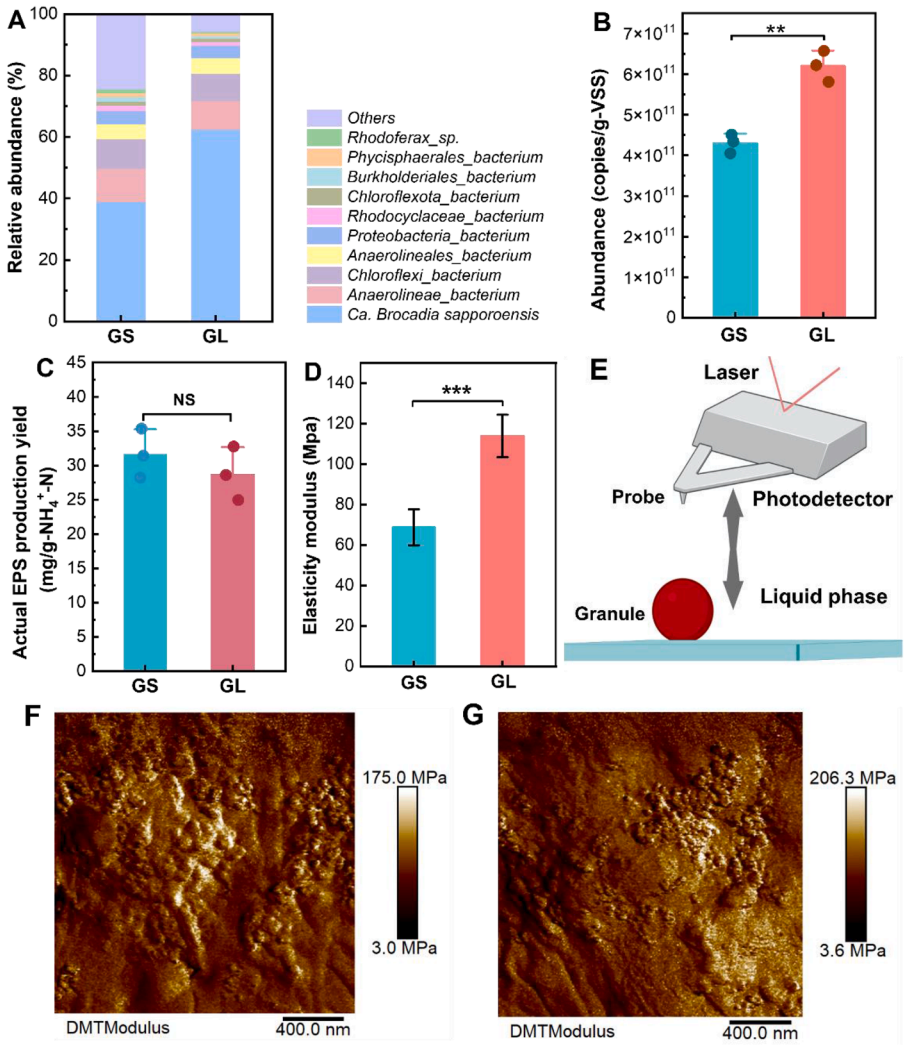

Fig. 3. Comparison of anammox abundance, EPS production and surface elastic modulus between S-Granules and L-Granules. Relative abundance of microbial communities detected by the metagenome sequencing (A) and the 16S rRNA gene copies of anammox bacteria (B) in S-Granules and L-Granules; Actual EPS production yields of S-Granules and L-Granules in 15-day incubation (C); Surface elastic modulus of S-Granules and L-Granules and its determination methods (D-G). Significant differences were detected using one-way analysis of variance: * $p<0.05$, ** $p<0.01$, and *** $p<0.001$.

(Fig. 4G). The surface of anammox bacterial cells were wrapped with the denser EPS (Fig. 4H, I), consistent with the higher EPS content in L-Granules (Figs. 1B, 4N). These encapsulated anammox bacterial cells were densely packed, with many cells being seriously deformed. Few dividing cells were observed in the vision field. These results suggest that anammox bacteria must compete with limited space, thus restricting their growth and division in L-Granules. The dense EPS with greater structural strength appeared to deform the cells and impede their growth. Overall, anammox bacteria in L-Granules were subjected to greater resistance and limited growth space, potentially resulting in lower bacterial growth yields.

To further confirm that the growth of anammox bacteria was restricted by the high structural strength of EPS, the bacterial membrane fluidity was assessed. Within a certain range, a higher membrane fluidity means an easier cell growth and division, and a lower polarization value indicates a better cell membrane fluidity (Wenzel et al., 2018; Mykytczuk et al., 2007). The overall bacterial polarization in L-Granules was significantly higher than that in S-Granules (-0.326 vs -0.348, $p<0.001$, Fig. S5), indicating poor membrane fluidity and limited bacterial growth ability in L-Granules.

Collectively, these results suggest that the external resistance raised by the EPS should be overcome for the division and reproduction of anammox bacteria. In S-Granules, the lower EPS content and less EPS strength resulted in less resistance, thus being beneficial for bacterial proliferation. Conversely, the higher EPS content and greater structural strength of L-Granules led to significant resistance.

3.4. *Effects of low-intensity ultrasound on anammox bacterial growth within granules*

To verify that the resistance caused by the dense EPS was indeed the primary factor leading to the sharp reduction of bacterial yield, low-intensity ultrasound was applied to treat L-Granules. This treatment can lead to the partial exfoliation and dissolution of EPS, without significantly affecting the granular structural stability (Yu et al., 2013; Xu et al., 2022). The optimal ultrasound parameter of 7.2 kJ/(g-VSS·cm^2) was determined by preliminary experiments (Fig. S6). Under this condition, no significant reduction in the proportion of viable cells in the granules was observed ($p>0.05$, Fig. S7).

The maximum specific ammonium removal rate of treated L-Granules showed a significant increase from 397.4 to 572.3 mg-NH_4^+-N/(g-VSS·d) ($p<0.01$, Table 1), indicating that low-intensity ultrasound can promote the anammox bacterial activities, which was in line with previous studies (Yu et al., 2013; Yang et al., 2023). Also, the growth yield

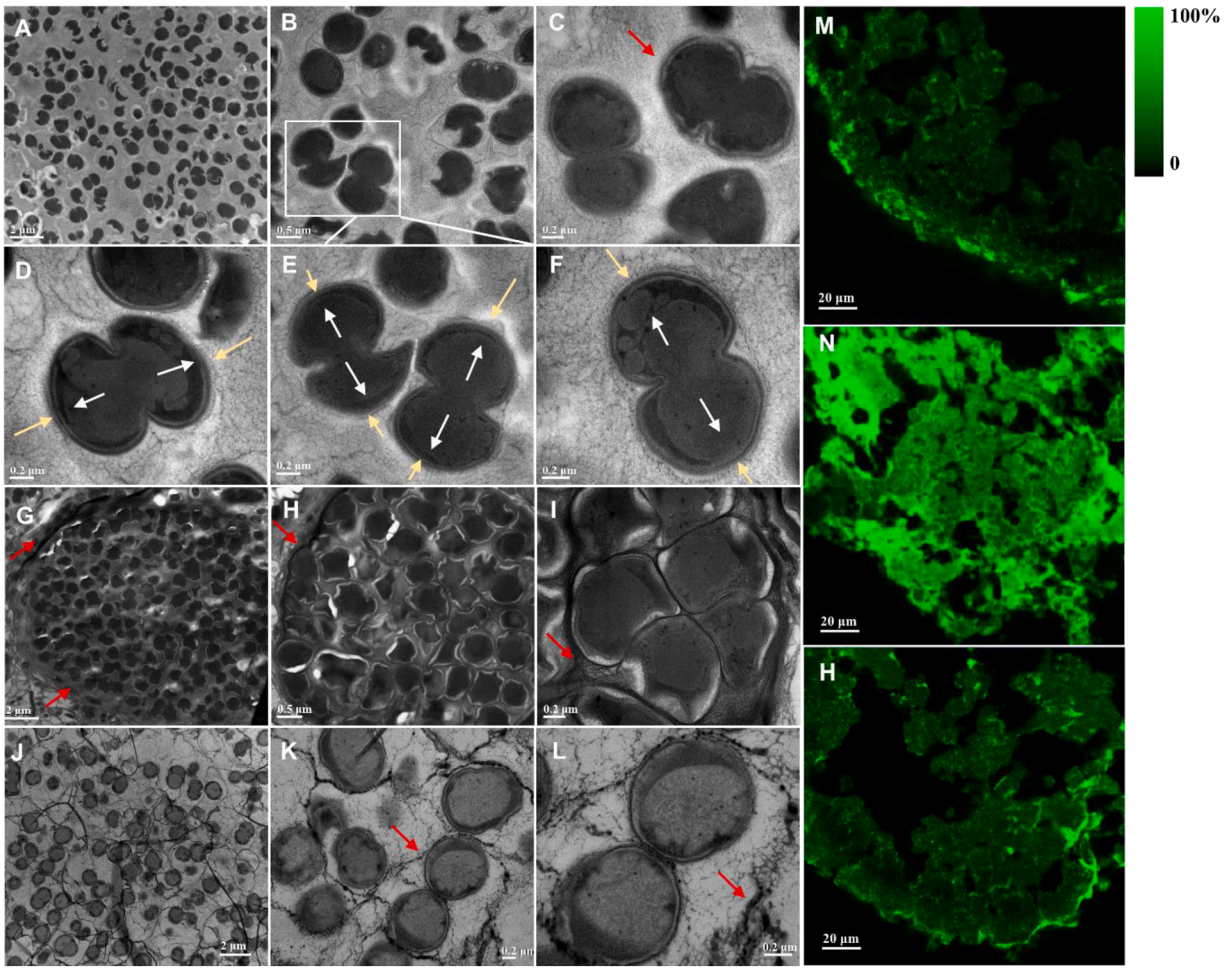

Fig. 4. Comparison of microstructure of granules and anammox bacterial cells among S-Granules, L-Granules and low-intensity ultrasound treated L-Granules. Microstructure of AnGS and anammox bacteria (A-L), and the distribution of extracellular proteins (M-H). A-F, G-I, and J-L refer to S-Granules, L-Granules and low-intensity ultrasound treated L-Granules, respectively; M, N, and H refer to S-Granules, L-Granules and low-intensity ultrasound treated L-Granules, respectively; The red arrow indicates the EPS around the cell, the white and yellow arrows indicate the bacterial division direction and the resistance direction of EPS, respectively; The green fluorescence indicate the extracellular proteins around cells.

Table 1
Nitrogen removal performance and anammox bacterial growth ability of L-Granules before and after ultrasonic treatment.

Parameters	L-Granules	Ultrasound-treated L-Granules	Variation rate (%)
Maximum specific ammonium removal rate (mg-NH_4^+-N/(g-VSS·d))	397.4 ±18.9	572.3±20.7	+44.0
Anammox bacterial growth yield [1] (g-C/g-NH_4^+-N)	(2.9±0.2) × 10^{-2}	(5.9±0.4) × 10^{-2}	+103.4
Maximum specific growth rate [1] (d^{-1})	(3.0±0.2) × 10^{-2}	(7.6±0.3) × 10^{-2}	+153.3
Doubling time [1] (d)	22.9±1.1	9.1±1.8	-60.3
Anammox bacterial growth yield [2] (copies/g-NH_4^+-N)	(4.8±3.4) × 10^{10}	(8.0±0.6) × 10^{10}	+66.7
Maximum specific growth rate [2] (d^{-1})	(3.1±0.2) × 10^{-2}	(7.1±0.2) × 10^{-2}	+129.0
Doubling time [2] (d)	22.3±1.6	9.8±1.6	-56.0

Note: Superscripts 1 and 2 refer to ^{13}C isotope-labelled culture experiments and qPCR-based quantification assay.

of anammox bacteria in treated L-Granules showed a significant increase from 2.9 × 10^{-2} to 5.9 × 10^{-2} g-C/g-NH_4^+-N (p<0.001). Consequently, the maximum specific growth rate increased substantially from 3.0 × 10^{-2} to 7.6 × 10^{-2} d^{-1} (p<0.001), accompanied by a significant reduction in anammox bacterial doubling time (p<0.001). Importantly, the results obtained by two different measurement methods (^{13}C isotope labelling and qPCR-based assay) were consistent (Table 1).

Further microstructural observations of the ultrasound treated L-Granules showed that the EPS surrounding anammox bacteria decreased obviously and the EPS structure became looser (Fig. 4J-L). Quantitative results showed that the EPS content in ultrasound-treated L-Granules significantly decreased from 244.2 to 183.1 mg/g-VSS (p<0.01). Specifically, the PN and PS contents decreased by 24.9% (p<0.001) and 25.3% (p<0.01), respectively (Fig. S8). The decline in green fluorescence intensity further indicated the decreased extracellular PN content around the cells after the ultrasound treatment (Fig. 4H). The FTIR spectrum results further demonstrated that the functional groups in EPS of L-Granules were almost unaffected by ultrasound treatment (Fig. S9), suggesting that ultrasound likely loosened the EPS structure and induced partial exfoliation and dissolution by disrupting intermolecular interactions (Xu et al., 2022). More interestingly, the deformed anammox bacteria cells became full and round, and a large number of dividing cells were observed, similar to previous observations in S-Granules. Since the identical low-intensity ultrasound had negligible effects on the growth yield of suspended anammox bacteria (Fig. S10), these results collectively prove that lowering the dense EPS surrounding the bacteria could enhance the growth yield of anammox bacteria. This also

confirmed that the resistance posed by the dense EPS in L-Granules was the primary cause for the low anammox bacterial growth yield.

4. Discussion

4.1. Low anammox bacterial growth yield leads to decreased maximum specific growth rate

The bacterial maximum specific growth rate is a critical parameter for understanding bacterial growth. The maximum specific growth rate of anammox bacteria equals to the product of maximum specific nitrogen removal rate and bacterial growth yield (Text S1) (Lotti et al., 2014; Zhang et al., 2017). Compared to S-Granules, L-Granules showed a higher specific nitrogen removal rate, which was reasonable in terms of the significantly higher abundance of anammox bacteria (Fig. 3A, B). Large granules typically develop through gradual growth of smaller ones, during which they experience a longer period of anammox bacterial enrichment. Therefore, large granules generally harbor a higher abundance of anammox bacteria compared to smaller ones (Kang et al., 2022). However, the anammox bacterial growth yield in L-Granules was much lower than in S-Granules (Fig. 2D). Therefore, despite the higher specific nitrogen removal rate of L-Granules, their maximum specific growth rate was significantly lower than S-Granules (Fig. 2E). This finding highlights that the growth yield of anammox bacteria in granules also plays a significant role, which may even overturn the impacts of maximum nitrogen removal activity.

4.2. Mechanical resistance of dense EPS reduced the bacterial growth yield in L-Granules

The only anammox bacteria species detected in both S-Granules and L-Granules was *"Ca. Brocadia sapporoensis"*. Also, endogenous anammox bacterial decay rates of S-Granules and L-Granules were 0.0013±0.0004 and 0.0014±0.0005 d^{-1}, respectively, which were comparable ($p>0.05$, Fig. S11). For the same anammox bacterial species, the energy obtained from converting a unit mass of nitrogen is theoretically constant, and the amount of anammox biomass produced should be constant as well (Basan et al., 2020; Kartal et al., 2012). Notably, the ATP content of anammox bacteria in L-Granules was significantly lower than that in S-Granules (Fig. S3). We speculated that energy generated by anammox bacteria in L-Granules might be diverted to other pathways, resulting in a significantly lower bacterial growth yield (Kartal et al., 2012). In fact, the actual EPS production yields of S-Granules and L-Granules showed no significant difference during the experimental period ($p>0.05$), indicating that the EPS synthesis was not the primary reason for the low anammox bacterial growth yield in L-Granules.

Further investigations showed that L-Granules exhibited the higher elastic modulus. Although the elastic modulus measured by AFM cannot precisely quantify the local mechanical resistance experienced by bacteria during cell division, it effectively reflects the relative differences in the overall structural strength of EPS within the granules. The higher structural strength of EPS in L-Granules caused anammox bacteria to be tightly wrapped and even severely deformed (Figs. 4G-I). Generally, bacteria generate traction forces during their growth and division. When the external resistance imposed by the network structure of EPS is low, cells can divide smoothly with relatively small traction forces. However, as the resistance increases, bacteria must exert stronger traction forces to sustain their growth (Saez et al., 2007). In this process, part of the energy may be consumed through cytoskeletal and protein-associated stress responses, thereby reducing the fraction of energy allocated to biomass synthesis (Flemming and Wingender, 2010; Even et al., 2017; Liu et al., 2022). This stress-induced energy redistribution could be a key factor contributing to the decrease in bacterial growth yield.

Notably, a substantial increase in the growth yield of anammox bacteria was observed in ultrasound treated L-Granules (Table 1). After ultrasonic treatment, the granular size and density remained unchanged (Fig. S12), indicating no significant increase in the overall internal space of granules. However, the EPS on the cell surface was properly eliminated and the EPS structure became looser, resulting in a relatively dispersed distribution of anammox bacteria. This alleviated the mechanical resistance posed on bacterial proliferation, thereby significantly enhancing the growth yield of anammox bacteria. Since low-intensity ultrasound had negligible effects on the growth yield of suspended anammox bacteria (Fig. S10), the increased anammox bacterial growth yield in ultrasound-treated L-Granules was primarily due to the alleviation of mechanical resistance imposed by the EPS matrix. Overall, our findings demonstrated that the dense EPS surrounding bacteria is a physical and mechanical barrier affecting cell division and population growth (Fig. S13).

Moreover, the specific nitrogen removal rate of ultrasound treated L-Granules was significantly promoted (Table 1). This can be attributed to the ultrasound-induced enhancement in granular mass transfer, as well as the promotion in anammox bacterial activity (Yu et al., 2013; Xu et al., 2022), both of which have been well documented previously. The increased specific nitrogen removal rate can also contribute to the growth rate of anammox bacteria. Our experiments highlighted that ultrasonic treatment could enhance the growth yield of anammox bacteria by lowering the dense EPS surrounding the cells, which has been largely overlooked in previous studies.

4.3. Implications of this study

In this study, we demonstrated that the reduced growth yield of anammox bacteria in large granules was a key factor contributing to their slow growth rate. Furthermore, we highlighted a critical yet largely overlooked mechanism: the physical and mechanical constraints imposed by the dense EPS content could significantly limit anammox bacterial proliferation and reduce their growth yield (Fig. S13).

The nitrogen removal performance of the anammox sludge bed reactor is closely linked to both the nitrogen removal rate and the granular biomass content (Tang et al., 2011). Increasing the biomass content is critical for intensifying nitrogen removal capacity, which relies on the growth of anammox bacteria within granules. In this study, L-Granules exhibited a higher nitrogen removal rate, yet their anammox bacterial growth rate was relatively low due to the limited growth yield. Since L-Granules accounted for the dominant fraction in the reactor, their slow growth rate implied a poor anammox biomass production rate. Therefore, promoting the growth rate of anammox bacteria within L-Granules would facilitate faster biomass production, and enhance the nitrogen removal capacity of the reactor. Also, the increased granular biomass can be used for seeding new anammox bioreactors.

Given that the enlargement of AnGS is typically associated with the elevated EPS content, applying appropriate hydrodynamic shear may effectively prevent excessive granular growth and mitigate the limitation effects of EPS secretion on bacterial proliferation. Moreover, a recent study showed that artificial disintegration and re-granulation of anammox sludge can produce granules with reduced overall EPS content (Jeong et al., 2025), thereby alleviating the mechanical resistance imposed on anammox bacterial growth, offering a potentially effective strategy to enhance biomass production. In addition, in practical applications, a portion of large-sized granules can be periodically collected for *ex-situ* low-intensity ultrasound treatment (Fig. S14) to moderately reduce EPS content without compromising the granule structural stability. The treated granules are then returned to the bioreactor to enhance sludge production.

5. Conclusions

In this study, the effects of EPS mechanical strength on the growth of anammox bacteria within granules were investigated. The major conclusions include:

1) Larger granules with a higher EPS content exhibited the higher maximum nitrogen removal activity but a lower bacterial growth yield, resulting in a significantly lower maximum specific growth rate, compared to smaller granules.
2) The EPS mechanical strength was significantly greater in large granules, in which the dense EPS matrix imposed a higher mechanical resistance, thereby limiting proliferation of anammox bacteria and reducing their growth yield.
3) Using low-intensity ultrasound to loosen EPS structure could improve the growth yield of anammox bacteria in large granules, and enhance nitrogen removal activity. These together contributed to a substantial increase in bacterial growth rate.

Overall, the findings highlight that physical and mechanical resistance imposed by high EPS contents plays a previously overlooked role in restricting anammox bacterial growth.

CRediT authorship contribution statement

Dongdong Xu: Writing – original draft, Visualization, Investigation, Data curation. **Tao Liu:** Writing – review & editing, Validation. **Jiahui Fan:** Methodology, Investigation, Data curation. **Wenda Chen:** Software, Resources, Formal analysis. **Yiyu Li:** Methodology, Investigation. **Meng Zhang:** Writing – review & editing, Resources, Funding acquisition. **Ping Zheng:** Writing – review & editing, Project administration. **Jianhua Guo:** Writing – review & editing, Validation, Supervision, Funding acquisition.

Declaration of competing interest

The authors declare that they have no known competing financial interests or personal relationships that could have appeared to influence the work reported in this paper.

Acknowledgement

This research was supported by the National Key Research and Development Program of China (2022YFC3203003), the Key Project of the Natural Science Foundation of Zhejiang Province (LZ23E080004). Jianhua Guo is supported by the Australian Research Council Discovery Project (DP230101340).

Supplementary materials

Supplementary material associated with this article can be found, in the online version, at doi:10.1016/j.watres.2025.124705.

Data availability

Data will be made available on request.

References

Baird, R., Rice, E., Eaton, A., 2017. Standard methods for the examination of water and wastewaters. Water Environment Federation, Chair Eugene W. Rice, American Public Health Association Andrew D. Eaton, American Water Works Association. 1, 71–90.
Basan, M., Honda, T., Christodoulou, D., Hörl, M., Chang, Y., Leoncini, E., Mukherjee, A., Okano, H., Taylor, B.R., Silverman, J.M., 2020. A universal trade-off between growth and lag in fluctuating environments. Nature 584 (7821), 470–474.
Boleij, M., Pabst, M., Neu, T.R., Van Loosdrecht, M.C., Lin, Y., 2018. Identification of glycoproteins isolated from extracellular polymeric substances of full-scale anammox granular sludge. Environ. Sci. Technol. 52 (22), 13127–13135.
Chaudhuri, O., Cooper-White, J., Janmey, P.A., Mooney, D.J., Shenoy, V.B., 2020. Effects of extracellular matrix viscoelasticity on cellular behaviour. Nature 584 (7822), 535–546.
Dsane, V.F., Jeon, H., Choi, Y., Jeong, S., Choi, Y., 2023. Characterization of magnetite assisted anammox granules based on in-depth analysis of extracellular polymeric substance (EPS). Bioresour. Technol. 369, 128372.
Even, C., Marlière, C., Ghigo, J., Allain, J., Marcellan, A., Raspaud, E., 2017. Recent advances in studying single bacteria and biofilm mechanics. Adv. Colloid. Interface. Sci. 247, 573–588.
Fu, L., Niu, B., Zhu, Z., Wu, S., Li, W., 2012. CD-HIT: accelerated for clustering the next-generation sequencing data. Bioinformatics 28 (23), 3150–3152.
Flemming, H., Wingender, J., 2010. The biofilm matrix. Nat. Rev. Microbiol. 8 (9), 623–633.
Hou, X., Liu, S., Zhang, Z., 2015. Role of extracellular polymeric substance in determining the high aggregation ability of anammox sludge. Water Res. 75, 51–62.
Jorba, I., Uriarte, J.J., Campillo, N., Farré, R., Navajas, D., 2017. Probing micromechanical properties of the extracellular matrix of soft tissues by atomic force microscopy. J. Cell. Physiol. 232 (1), 19–26.
Jeong, S., Dsane, V.F., Choi, Y., 2025. Effects of granule disintegration and re-granulation on the physiological characteristics and microbial diversity of anammox granules. Chemosphere 370, 143979.
Kartal, B., Kuenen, J.V., Van Loosdrecht, M., 2010. Sewage treatment with anammox. Science 328 (5979), 702–703.
Kartal, B., van Niftrik, L., Keltjens, J.T., den Camp, H.J.O., Jetten, M.S., 2012. Anammox—growth physiology, cell biology, and metabolism. Adv. Microb. Physiol. 60, 211–262.
Kang, D., Zheng, P., Li, W., Xu, D., Chen, W., Pan, C., 2022. Stratification patterns of anammox granular sludge bed: Linking particle size distribution to microbial activity and community. Environ. Res. 210, 112763.
Liu, Y.Q., Liu, Y., Tay, J.H., 2005. Relationship between size and mass transfer resistance in aerobic granules. Lett. Appl. Microbiol. 40 (5), 312–315.
Liu, Y., Tay, J., 2004. State of the art of biogranulation technology for wastewater treatment. Biotechnol. Adv. 22 (7), 533–563.
Liu, T., Duan, H., Lücker, S., Zheng, M., Daims, H., Yuan, Z., Guo, J., 2024. Sustainable wastewater management through nitrogen-cycling microorganisms. Nat. Water 2, 936–952.
Li Wong, L., Lu, Y., Ho, J., Mugunthan, S., Law, Y., Conway, P., Kjelleberg, S., Seviour, T., 2023. Surface-layer protein is a public-good matrix exopolymer for microbial community organisation in environmental anammox biofilms. The ISME J. 17 (6), 803–812.
Lin, X., Wang, Y., 2017. Microstructure of anammox granules and mechanisms endowing their intensity revealed by microscopic inspection and rheometry. Water Res 120, 22–31.
Li, Q., Chen, J., Liu, G., Xu, X., Zhang, Q., Wang, Y., Yuan, J., Li, Y., Qi, L., Wang, H., 2021. Effects of biotin on promoting anammox bacterial activity. Sci. Rep. 11 (1), 2038.
Li, R., Li, Y., Kristiansen, K., Wang, J., 2008. SOAP: short oligonucleotide alignment program. Bioinformatics 24 (5), 713–714.
Lotti, T., Kleerebezem, R., Lubello, C., van Loosdrecht, M.C., 2014. Physiological and kinetic characterization of a suspended cell anammox culture. Water Res. 60, 1–14.
Liu, X., Inda, M.E., Lai, Y., Lu, T.K., Zhao, X., 2022. Engineered living hydrogels. Adv. Mater. 34 (26), 2201326.
Lawson, C.E., Wu, S., Bhattacharjee, A.S., Hamilton, J.J., McMahon, K.D., Goel, R., Noguera, D.R., 2017. Metabolic network analysis reveals microbial community interactions in anammox granules. Nat. Commun. 8 (1), 15416.
Mykytczuk, N., Trevors, J.T., Leduc, L.G., Ferroni, G.D., 2007. Fluorescence polarization in studies of bacterial cytoplasmic membrane fluidity under environmental stress. Progr. Biophys. Mol. Biol. 95 (1-3), 60–82.
Mishima, K., Nakamura, M., 1991. Self-immobilization of aerobic activated sludge–a pilot study of the aerobic upflow sludge blanket process in municipal sewage treatment. Water Sci. Technol. 23 (4-6), 981–990.
Peng, Y., Leung, H.C., Yiu, S., Chin, F.Y., 2012. IDBA-UD: a de novo assembler for single-cell and metagenomic sequencing data with highly uneven depth. Bioinformatics 28 (11), 1420–1428.
Peng, M., Chen, Y., Chen, Y., Sun, W., Liu, M., Weng, X., Wang, S., Shen, Y., Fu, H., 2025. Nondestructive three-dimensional structure and growth characteristics of anammox granular sludge. Int. Biodeterior. Biodegrad. 198, 105986.
Pronk, M., De Kreuk, M.K., De Bruin, B., Kamminga, P., Kleerebezem, R.V., Van Loosdrecht, M., 2015. Full scale performance of the aerobic granular sludge process for sewage treatment. Water Res 84, 207–217.
Saraswathibhatla, A., Indana, D., Chaudhuri, O., 2023. Cell–extracellular matrix mechanotransduction in 3D. Nat. Rev. Mol. Cell Biol. 24 (7), 495–516.
Saez, A., Ghibaudo, M., Buguin, A., Silberzan, P., Ladoux, B., 2007. Rigidity-driven growth and migration of epithelial cells on microstructured anisotropic substrates. Proc. Natl. Acad. Sci. 104 (20), 8281–8286.
Tang, C., Zheng, P., Wang, C., Mahmood, Q., Zhang, J., Chen, X., Zhang, L., Chen, J., 2011. Performance of high-loaded ANAMMOX UASB reactors containing granular sludge. Water Res 45 (1), 135–144.
Van Niftrik, L., Geerts, W.J., Van Donselaar, E.G., Humbel, B.M., Webb, R.I., Harhangi, H.R., Camp, H.J.O.D., Fuerst, J.A., Verkleij, A.J., Jetten, M.S., 2009. Cell division ring, a new cell division protein and vertical inheritance of a bacterial organelle in anammox planctomycetes. Mol. Microbiol. 73 (6), 1009–1019.
Wilén, B., Liébana, R., Persson, F., Modin, O., Hermansson, M., 2018. The mechanisms of granulation of activated sludge in wastewater treatment, its optimization, and impact on effluent quality. Appl. Microbiol. Biotechnol. 102, 5005–5020.
Wang, S., Liu, L., Li, H., Fang, F., Yan, P., Chen, Y., Guo, J., Ma, T., Shen, Y., 2020a. The branched chains and branching degree of exopolysaccharides affecting the stability of anammox granular sludge. Water Res. 178, 115818.
Wang, W., Liu, Q., Xue, H., Wang, T., Fan, Y., Zhang, Z., Wang, H., Wang, Y., 2022. The feasibility and mechanism of redox-active biochar for promoting anammox performance. Sci. Total Environ. 814, 152813.

Wenzel, M., Vischer, N.O., Strahl, H., Hamoen, L.W., 2018. Assessing membrane fluidity and visualizing fluid membrane domains in bacteria using fluorescent membrane dyes. Bio-Protocol 8 (20), e3063.
Wang, X., Yang, H., Su, Y., Liu, X., 2020b. Characteristics and mechanism of anammox granular sludge with different granule size in high load and low rising velocity sewage treatment. Bioresour. Technol. 312, 123608.
Weiss, D.S., 2004. Bacterial cell division and the septal ring. Mol. Microbiol. 54 (3), 588–597.
Xu, D., Fan, J., Li, W., Chen, W., Pan, C., Kang, D., Li, Y., Shan, S., Zheng, P., 2021. Deciphering correlation between permeability and size of anammox granule: "pores as medium. Water Res 191, 116832.
Xu, D., Fan, J., Chen, W., Pan, C., Jiang, L., Kang, D., Li, W., Ding, S., Zheng, P., Hu, B., 2022. Insights into the enhanced effect of Low-Intensity Ultrasound on anammox granular sludge by relieving the embolism. Chem. Eng. J. 446, 137470.
Yang, X., Li, H., Nie, S., Su, JQ., Weng, B., Zhu, G., 2015. Potential contribution of anammox to nitrogen loss from paddy soils in Southern China. Appl Environ Microbiol 81, 938–947.
Yang, J., Zhu, Y., Xie, Y., Tian, S., Zhang, G., Zhang, C., 2023. Effects of low-intensity ultrasound on anammox granular sludge. J. Water Process. Eng. 53, 103795.
Yu, J., Chen, H., Zhang, J., Ji, Y., Liu, Q., Jin, R., 2013. Enhancement of ANAMMOX activity by low-intensity ultrasound irradiation at ambient temperature. Bioresour. Technol. 142, 693–696.
Zhao, Y., Feng, Y., Zhou, J., Zhang, K., Sun, J., Wang, L., Liu, S., 2023. Potential bacterial isolation by dosing metabolites in cross-feedings. Water Res 231, 119589.
Zhang, L., Narita, Y., Gao, L., Ali, M., Oshiki, M., Okabe, S., 2017. Maximum specific growth rate of anammox bacteria revisited. Water Res 116, 296–303.